

# Gain and Loss in Quantum Cascade Lasers

A. Wacker and S.-C. Lee

*Institut für Theoretische Physik, Technische Universität Berlin, 10623 Berlin, Germany*

---

## Abstract

We report gain calculations for a quantum cascade laser using a fully self-consistent quantum mechanical approach based on the theory of nonequilibrium Green functions. Both the absolute value of the gain as well as the spectral position at threshold are in excellent agreement with experimental findings for  $T = 77\text{K}$ . The gain strongly decreases with temperature.

*Key words:* quantum cascade lasers, gain, quantum transport

*PACS:* 42.55.Px, 05.60.Gg, 73.40.-c

---

## 1 Introduction

Quantum cascade lasers (QCL) [1] constitute an important source of midinfrared radiation. These complex semiconductor heterostructures exhibit a sequence of several ( $\sim 30$ ) periods. Each period consists of an active region, where the optical transition takes place, and an injector region guiding the electrons from the lower level into the upper level of the active region in the neighboring period in a certain bias range.

The operation of QCLs is based on a complex interplay between tunneling through injector regions, scattering transitions, and the interaction with the infrared light. While semiclassical theories based on the Boltzmann equation [2] can explain several features of the relaxation processes in the active region, a quantum transport treatment is indispensable to study the functionality of the injector as well as its interplay with the active region. Such transport simulations have been performed very recently applying nonequilibrium Green functions [3,4] and density matrix theory [5] for the QCL. Besides the transport properties, the gain spectrum is also strongly affected by scattering processes. While these effects are commonly taken into account by means of phenomenological broadening, we present a full self-consistent quantum mechanical description here.

We model the transport in QCLs employing the technique of nonequilibrium Green functions [6]. The quantum kinetic equations are solved using self-energies in the self-consistent Born approximation for phonon and impurity scattering. The interaction with the microwave field is treated within linear response with respect to the *nonequilibrium state*. In this way, we obtain the complex dielectric susceptibility and the gain coefficient  $g$ . This provides us with a self-consistent formalism combining scattering and coherent evolution, which provides level occupations and broadening of optical spectra within a single approach. As an example we present results for the GaAs/AlGaAs structure of Ref. [7].

## 2 The model

We set up our Hamiltonian within the basis of Wannier-functions, which allows for a direct calculation from nominal sample parameters using standard envelope functions (see [8] for details). The self-energies for phonon and interface roughness scattering are taken into account within the self-consistent Born approximation. The solution of the Kadanoff-Baym equations [6] provides us with the lesser and retarded Green functions

$$\mathbf{G}^{</ret}(\mathbf{k}, t_1, t_2) = \int \frac{dE}{2\pi} \mathbf{G}^{</ret}(\mathbf{k}, E) e^{-iE(t_1-t_2)/\hbar} \quad (1)$$

in the nonequilibrium state (a stationary state, thus the Green functions only depend on the time difference  $t_1 - t_2$ ). Here bold-face capital letter describe matrices  $G_{mn}^{\mu\nu}$ , where  $\nu$  is the band index and  $n$  the period index in the QCL of the respective Wannier functions  $\Psi_n^\nu(z)$ .  $\mathbf{k}$  denotes a two-dimensional wave vector, describing the free-particle behavior in the plane perpendicular to the growth direction. Details are given in Ref. [4], where this approach was applied to the calculation of the current-field relation in good agreement with the experimental values.

Now we consider the coupling to an external optical field  $F$  (in  $z$  direction) with the vector potential  $\vec{A}(t) = \frac{1}{i\omega} \int \frac{d\omega}{2\pi} F(\omega) e^{-i\omega t} \vec{e}_z$  which provides us with the perturbation potential  $\delta\hat{U}(t) = -\frac{e}{m_e} \vec{A} \cdot \hat{\vec{p}}$  in the Hamiltonian (neglecting quadratic terms). Its matrix representation reads  $\delta\mathbf{U}(t) = \int d\omega / (2\pi) \delta\mathbf{U}(\omega) e^{-i\omega t}$  with

$$\delta U_{n,m}^{\nu\mu}(\omega) = -\frac{e}{\hbar\omega} F(\omega) \langle \Psi_n^\nu | \frac{\hbar}{i} \hat{p}_z | \Psi_m^\mu \rangle. \quad (2)$$

Here  $\hat{p}$  is the momentum operator and  $m_e$  is the electron mass.

We linearize the time-dependent Kadanoff-Baym equations with respect to  $\delta\mathbf{U}(t)$  around the nonequilibrium state (1). Applying the Fourier representation

$$\delta\mathbf{G}(\mathbf{k}, t_1, t_2) = \int \frac{d\omega}{2\pi} e^{-i\omega t_1} \int \frac{dE}{2\pi} \delta\mathbf{G}(\mathbf{k}, \omega, E) e^{-iE(t_1-t_2)/\hbar}, \quad (3)$$

the field-induced change of Green functions is given by

$$\begin{aligned}\delta\mathbf{G}^<(\mathbf{k}, \omega, E) &= \mathbf{G}^{\text{ret}}(\mathbf{k}, E + \hbar\omega)\delta\mathbf{U}(\omega)\mathbf{G}^<(\mathbf{k}, E) \\ &+ \mathbf{G}^<(\mathbf{k}, E + \hbar\omega)\delta\mathbf{U}(\omega)\mathbf{G}^{\text{adv}}(\mathbf{k}, E).\end{aligned}\quad (4)$$

In general, the self-energies also change due to the perturbation, which gives more terms of the same order. This corresponds to ladder corrections, which are neglected here.

From the lesser Green function we obtain the change in current density:

$$\begin{aligned}\delta J(t) &= \frac{e}{LA}\delta\langle\frac{\hat{p}_z}{m_e}\rangle \\ &= \frac{2(\text{for spin})e}{dA\text{i}}\sum_{\mathbf{k}, n, \mu, \nu}\langle\Psi_0^\nu|\frac{\hat{p}_z}{m_e}|\Psi_n^\mu\rangle\delta G_{n,0}^{\mu\nu<}(\mathbf{k}; t, t)\end{aligned}\quad (5)$$

where scattering induced currents have been neglected. Here  $A$  is the cross section,  $L$  is the total length, and  $d$  is the period of the sample. The Fourier transform  $\delta J(\omega)$  provides us with the Polarization  $\delta P(\omega) = \text{i}\frac{\delta J(\omega)}{\omega}$  and the complex susceptibility  $\chi(\omega) = \frac{P(\omega)}{\varepsilon_0 F(\omega)}$ . From standard electrodynamics (see, e.g., Sec. 7.5 of [9]) we obtain the gain coefficient (for low absorption or gain)

$$g(\omega) \approx -\frac{\omega}{c}\frac{\Im\{\chi(\omega)\}}{\sqrt{\varepsilon_r + \Re\{\chi(\omega)\}}}\quad (6)$$

where  $\varepsilon_r = 13$  is the static dielectric susceptibility of GaAs. Note that all quantities entering the calculation are material parameters.

### 3 Results

We have applied the above formalism to the GaAs/AlGaAs structure reported in Ref. [7]. Fig. 1 shows absorption and gain spectra at 77 K calculated for different applied bias, ranging from 0 to 0.24 V/period (0.1 V/period  $\sim$  22 kV/cm). At zero bias, there is only absorption with a strong absorption line at around 138 meV. As the applied voltage increases there is an overall decrease in absorption and a blue shift of the absorption peak. At around 0.14 V/period or 1 kA/cm<sup>2</sup>, there is a transition to gain at around 120 meV. From then on, as the voltage increases, the gain increases further, accompanied by a shift of the peak gain to higher frequencies. A double peaked structure also appears in the gain structure. At present, we have not yet made a detailed analysis of the spectra, and we cannot definitely assign the absorption or gain features, and shifts in these features, to specific transitions in the structure. We can, however, obtain some understanding of the transition from absorption to gain if we consider the populations of the Wannier levels. Fig. 2(a)

shows the Wannier levels in one period of the structure, and Fig. 2(b) shows the populations in each of these levels as the voltage is increased. At zero bias, all the population is in the lowest Wannier level which is localized in the active region. As the voltage increases, the population moves out of this level into the next two higher levels which are partially in the active region and partially in the injector, and with yet further voltage increase, the population moves into the fourth and fifth levels which are localized mainly in the injector. Finally, above 0.25 V/period we see a large population inversion with the population lying mainly in injector levels and in the highest Wannier level in the active region, and with almost no population in the lowest level. The transition from absorption to gain occurs between 0.15 to 0.2 V/period. This is also the point where the population in the excited level in the active region first exceeds the population in the lowest level. Thus, with this picture we can follow the movement of the carriers across the period from the lowest level in the active region, through the injector, and into the highest level in the active region as the applied voltage increases. This movement can be related to the shift and realignment of the Wannier levels as the voltage changes.

In Fig. 3(a), we show gain and absorption spectra calculated for 300 K. The main differences compared with the spectra at 77 K, are that the absorption and gain are reduced by a factor of more than two at 300 K, compared with their values at 77 K, for the same current density. The width of the spectra is also wider at the higher temperature. Both these effects can be understood if we consider the populations of the Wannier levels at 300 K shown in Fig. 3(b). The figure shows that the population is much more widely distributed over the different levels at higher temperature. There is a significant proportion of the population in higher levels even for zero bias, unlike the case at 77 K where the population is mainly in the lowest level. Similarly, in the case of population inversion at higher voltage, there is a larger fraction of the population in the lowest level at 300 K than at 77 K. Hence, because the population difference between different levels is reduced at higher temperature, this causes a reduction in the absorption or gain. The redistribution of carriers over more levels allows more transitions to occur and this, together with the increased phonon scattering, explains the larger width of the spectra at 300 K compared to 77 K.

## 4 Discussion

We have presented gain calculations for the QCL of Ref. [7] using a fully self-consistent quantum mechanical approach on the basis of nonequilibrium Green functions. We find that gain sets in for current densities around  $1 \text{ kA/cm}^2$  and increases with current. For  $T = 77 \text{ K}$ , the peak gain coefficient is  $60 \text{ cm}^{-1}$  at  $7 \text{ kA/cm}^2$  and a photon energy of 130 meV, in excellent agreement with the findings of Ref. [7] (material gain  $G_M = 63 \text{ cm}^{-1}$  at threshold  $J_{\text{th}} = 7.2 \text{ kA/cm}^2$ ). The spectral position of the gain spectrum agrees well with the findings of Ref. [10] although

neither a double peak structure nor a blue shift was resolved in the experiment. For room temperature, the gain is significantly reduced and becomes less than the estimated loss explaining the lack of lasing operation.

For practical reasons, the influence of electron-electron scattering has been neglected in these calculations. While the current density seems not to depend strongly on the type of scattering mechanism (see the discussion in [4]), electron-electron interaction may affect the gain spectrum. This constitutes an important issue for future research.

We thank A. Knorr and M. Pereira for helpful discussions. Financial support by DFG through FOR394 is gratefully acknowledged.

## References

- [1] J. Faist *et al.*, *Science* **264**, 553 (1994), G. Scamarcio *et al.*, *Appl. Phys. Lett.* **70**, 1796 (1997), G. Strasser *et al.*, *Appl. Phys. Lett.* **75**, 1345 (1999).
- [2] S. Tortora, F. Compagnone, A. Di Carlo, and P. Lugli, *Physica E* **7**, 20 (2000), R. C. Iotti and F. Rossi, *Appl. Phys. Lett.* **78**, 2902 (2001).
- [3] A. Wacker, in *Advances in Solid State Physics*, edited by B. Kramer (Springer, Berlin, 2001), p. 199.
- [4] S.-C. Lee and A. Wacker, *Physica E*, to be published.
- [5] R. C. Iotti and F. Rossi, *Phys. Rev. Lett.*, in press.
- [6] H. Haug and A.-P. Jauho, *Quantum Kinetics in Transport and Optics of Semiconductors* (Springer, Berlin, 1996).
- [7] C. Sirtori *et al.*, *Appl. Phys. Lett.* **73**, 3486 (1998).
- [8] A. Wacker, *Phys. Rep.* (2001), in press.
- [9] J. D. Jackson, *Classical Electrodynamics*, 3 ed. (John Wiley & Sons, New York, 1998).
- [10] F. Eickemeyer *et al.*, *Appl. Phys. Lett.* **76**, 3254 (2000).

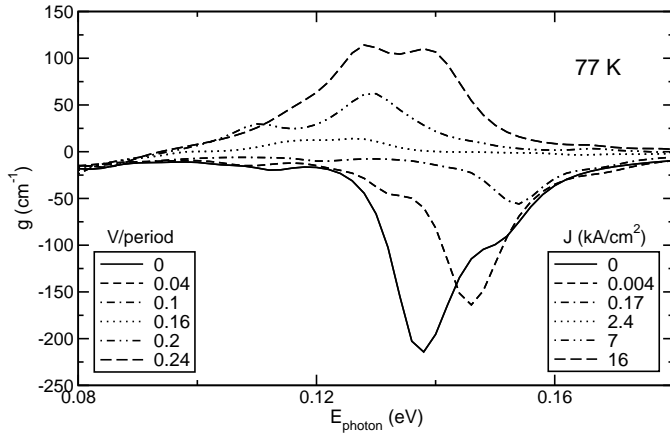


Fig. 1. Calculated gain and absorption ( $g < 0$ ) spectra for the QCL from [7]. Data for different voltage drops per period and corresponding current densities are displayed.

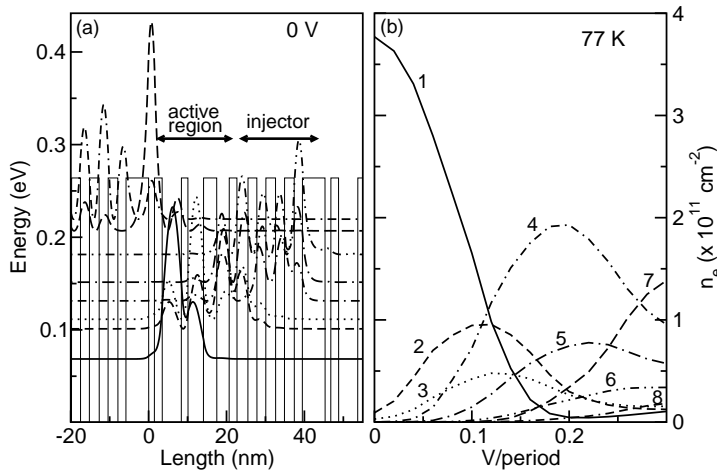


Fig. 2. (a) Square of Wannier functions associated with one period together with the band alignment. (b) Population of the Wannier levels shown in (a) as a function of voltage drop for  $T = 77$  K. The curves are labelled according to increasing energy, i.e. curve 1 shows the population of the Wannier level with the lowest energy.

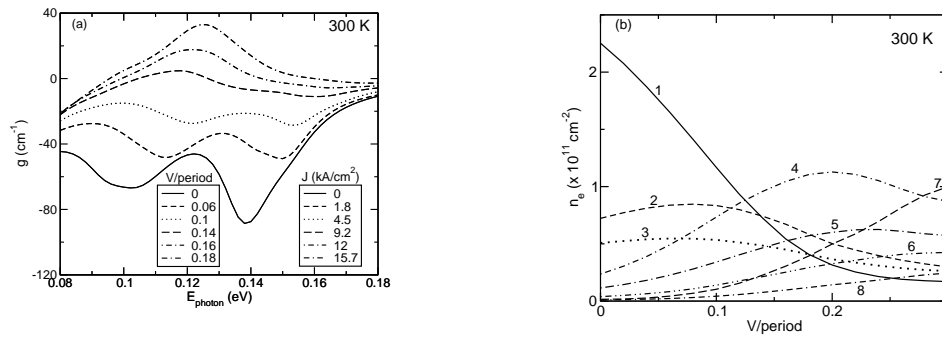


Fig. 3. (a) Calculated gain and absorption ( $g < 0$ ) spectra for 300 K; (b) population of the Wannier levels as a function of voltage drop. The curves are labelled as in Fig. 2(b).